Interannual Variations of the Blocking High over the Ural Mountains and Its Association with the AO/NAO in Boreal Winter

LI Chao[2,3](李 超), ZHANG Qingyun[1,2*](张庆云), JI Liren[1,2](纪立人), and PENG Jingbei[2](彭京备)

1 *State Key Laboratory of Numerical Modeling for Atmospheric Sciences and Geophysical Fluid Dynamics, Institute of Atmospheric Physics, Chinese Academy of Sciences, Beijing* 100029

2 *International Center for Climate and Environment Sciences, Institute of Atmospheric Physics, Chinese Academy of Sciences, Beijing* 100029

3 *Graduate University of the Chinese Academy of Sciences, Beijing* 100049

(Received May 7, 2011; in final form September 25, 2011)

ABSTRACT

This paper analyzes interannual variations of the blocking high over the Ural Mountains in the boreal winter and their association with the Arctic Oscillation/North Atlantic Oscillation (AO/NAO). In January, the relationship between the Ural blocking high (UR) and the AO index is statistically significant. The UR tends to occur more frequently and with greater strength during negative AO periods. Some strong URs also occur during positive AO phases (positive UR-AO events), as in January 2008. This paper discusses the characteristics of atmospheric circulation in the cases of positive UR-AO events and contrast cases (negative UR-AO events). The eastward extending of the Icelandic Low (IL) center and the associated NAO dipole anomaly pattern in the upstream region may play a more important role for the UR-AO events. When the center of the IL shifts eastward to 30°W, the amplitude of zonal wavenumber 2 (wavenumber 3) is intensified in the positive (negative) UR-AO events, which favors positive (negative) height anomalies over the Urals. Further analyses indicate that the intensified zonal wind in high latitudes and weakened zonal wind in midlatitudes over the North Atlantic Ocean render the eastward shift of the IL and the NAO dipole anomaly pattern. The Ural blocking in January 2008 bears similar characteristics to the positive UR-AO events.

Key words: Ural blocking high, AO, NAO dipole anomaly pattern, Icelandic Low

Citation: Li Chao, Zhang Qingyun, Ji Liren, et al., 2012: Interannual variations of the blocking high over the Ural Mountains and its association with the AO/NAO in boreal winter. *Acta Meteor. Sinica*, **26**(2), 163–175, doi: 10.1007/s13351-012-0203-3.

1. Introduction

Certain large-scale flow patterns typically persist beyond the periods associated with synoptic-scale variability in the extratropics (Dole, 1986). Two of the most frequently described and discussed phenomena are blocking (e.g., Rex, 1950; Sumner, 1954) and teleconnection (e.g., Wallace and Gutzler, 1981; Barnston and Livezey, 1987).

Atmospheric blocking is one of the most important weathers in midlatitudes and has long been recognized as a physical process of profound dynamical interest and of great practical relevance to operational forecasting (Tibaldi and Molteni, 1990). The region around the Ural Mountains is the third preferred region for blocking occurrence associated with the Mediterranean storm track (Dole and Gordon, 1983; Wang et al., 2010). The circulation anomalies over this sector have important effects on the East Asian weather and climate (Tao, 1957; Ye et al., 1962). A strong positive height anomaly over the Urals in winter is related to a colder surface temperature in

Supported by the China Meteorological Administration Special Public Welfare Research Fund (GYHY201106015), National Science and Technology Support Program of China (2009BAC51B02), National Basic Research and Development (973) Program of China (2009CB421401), and National Natural Science Foundation of China (40975022).

*Corresponding author: zqy@mail.iap.ac.cn.

East Asia (Li, 2004). If the blocking high over the Urals persists, the long-lasting anomalies associated with the blocking would be responsible for the extreme events. For example, severe snowstorms occurred across China in January 2008 while a long-lived blocking high occurred over the Urals (the "0801" event, hereafter). Recently, Wang et al. (2010) found that the Ural blocking has exerted more influences on the East Asian winter climate following the climate shift in the mid 1970s. The circulation pattern over the Urals is one of the critical factors in winter seasonal prediction for East Asia (Li, 2004), making very important to understand it the variability of the Ural blocking high.

The relation between blocking and teleconnection patterns has been widely investigated (e.g., Dole, 1986; Wiedenmann et al., 2002; Barriopedro et al., 2006). As previously indicated, blocking high and teleconnection are the most prominent persistent anomalies, and both phenomena share some common features, including a two-week time period and intriguing structural similarities. The Arctic Oscillation (AO) and North Atlantic Oscillation (NAO) are two of the most important teleconnection patterns in mid-high latitudes. The AO represents the leading empirical orthogonal function of a winter sea level pressure (SLP) field and has a zonal symmetrical appearance associated with the polar vortex. The NAO represents the difference between the Icelandic Low (IL) and the Azores High (AH) as normalized monthly mean SLP anomalies and has a more local dipole structure. The regional weather and climate over East Asia are greatly influenced by the variability of AO/NAO and by the Ural blocking. Park et al. (2011) noted that the cold surge over East Asia associated with blocking tends to occur during negative AO periods. Because the Ural blocking is one of the most important weather systems over East Asia, the relation between this system and the AO/NAO deserves a further study. In recent years, many investigations observed an eastward shift of the center of action of the NAO since the late 1970s (Hilmer and Jung, 2000). We should concern not only the index and phase of the AO/NAO, but also the structure of the teleconnections. As for the impacts of AO/NAO anomaly patterns, we have a paucity of knowledge.

This study discusses the interannual variability of the Ural blocking and its relation to the AO/NAO. Section 2 describes the data and analysis methods used in this study. Section 3 details the interannual variability of the Ural blocking and its influence on the East Asian climate. Section 4 presents the statistical relationship between the AO/NAO and the Ural blocking, and then describes the circulation anomaly features associated with the Ural blocking in some abnormal years. Section 5 documents some possible explanations for the circulation anomaly features. The summary and discussion are given in Section 6.

2. Data and methods

The reanalysis data used in the present study are from the National Centers for Environmental Prediction-National Center for Atmospheric Research (NCEP-NCAR) (Kalnay et al., 1996). Variables analyzed include the monthly mean geopotential height, surface air temperature (SAT), zonal wind, and daily geopotential height from January 1960 to December 2008. The data are on a 2.5°×2.5° horizontal resolution and extend from 1000 to 10 hPa at 17 vertical pressure levels. The AO and NAO indices (AOI and NAOI) are taken from the Climate Prediction Center of NCEP.

The blocking index of Tibaldi and Molteni (1990) (TM90, hereafter) is used here to examine the interannual variation of the Ural blocking. The TM90 index is defined based upon two values of daily 500-hPa geopotential height gradient evaluated at each longitude,

$$\mathrm{GHGS} = \frac{Z(\phi_0) - Z(\phi_s)}{\phi_0 - \phi_s},$$
$$\mathrm{GHGN} = \frac{Z(\phi_n) - Z(\phi_0)}{\phi_n - \phi_0},$$

where ϕ_n=80°+Δ, ϕ_0=60°+Δ, ϕ_s=40°+Δ, and Δ = –5°, 0°, or 5°. A given longitude is defined as "blocked" if the following conditions are satisfied for at least one of the three values of Δ: GHGS > 0, GHGN < –10 m (deg lat)$^{-1}$. The maximum value of GHGS here is used to estimate the amplitude of blocking (Tibaldi and Molteni, 1990).

To identify the characteristics of the quasi-stationary planetary wave, we apply zonal Fourier harmonics to the geopotential height. By expanding the monthly mean fields into their zonal Fourier harmonics, the zonal wavenumbers 1–3 are used to represent a quasi-stationary planetary wave following the method of van Loon et al. (1973).

The time period analyzed is from 1960 to 2008. We use January monthly mean to represent the boreal winter and contrast it with the "0801" event, and the winter of 2008 refers to only January 2008. In this study, the climatology mean is defined as the average from 1960 to 2008, and the anomaly is the departure from this climatology mean. Two-sided Student's t-tests are applied to test the significance of the composites and correlations.

3. Interannual variability of the Ural blocking and its possible impact on the East Asian winter climate

The activity of the blocking high over the Eurasian sector (0°–90°E) is characterized by obvious seasonal variability and interannual variability (Barriopedro et al., 2006). In this section, we first describe the definition and interannual variability of the Ural blocking high and then its possible impact on the winter climate over East Asia.

A positive (negative) anomaly of 500-hPa height over the Ural Mountains represents enhanced (weakened) blocking activity over this sector (Li, 2004). Li (2004) used a normalized height anomaly at the key point (60°N, 60°E) to represent the circulation anomaly over the Urals. Li and Gu (2010) used area averaged (45°–65°N, 40°–70°E) monthly mean geopotential height anomalies at 500 hPa as the index of the Ural high (UHI). The geopotential height and geopotential height anomaly at 500 hPa are used to estimate the activity of blocking. Many blocking detection methods employ daily 500-hPa geopotential height (e.g., TM90) or daily 500-hPa geopotential height anomaly (e.g., Dole and Gordon, 1983) as the base fields.

In this study, we use the area averaged (50°–70°E) TM90 index to represent the blocking activity over the Urals. Figure 1 illustrates the interannual variations of the Ural blocking frequency (URBF) and amplitude (URBA). The interannual variation of URBA is highly consistent with that of URBF, the variation of which is discussed subsequently. Meanwhile, the correlation coefficient of UHI and URBF is 0.415, which exceeds the 99% confidence level. The high correlation implies that UHI can also express some features of the Ural blocking. If there was an open ridge or cyclone over the Urals in a nonblocked event, the TM90 index would not distinguish the difference among atmospheric circulation anomaly patterns. The UHI is another supplemental tool that identifies the characteristics of circulation anomalies over the Urals, especially for the nonblocked events.

We then investigate the possible impact of the Ural blocking on the winter climate over East Asia. Figure 2 displays the composite SAT of the months in which the URBF is greater than 0.16 (approximately 5 days). A significant negative SAT anomaly dominates the eastern part of China, possibly associated with the activity of the Ural blocking. The Ural blocking would induce anomalous cold temperature anomalies downstream of the blocking high due to the northerly advection by the anomalous meridional flow. Thus, it is very important to explore the relationship between the Ural blocking and related driving factors.

4. The interannual relationship between the AO/NAO and the Ural blocking high

Though many previous studies have explored the influence of teleconnection patterns on the blocking high, the relation remains unclear. Considering the impact of the AO/NAO on the East Asian winter monsoon (e.g., Gong et al., 2001; Wu and Wang, 2002; Chen et al., 2005), the relation between the AO/NAO and the Ural blocking deserves attention. In January, the correlation coefficient of the AOI and NAOI is 0.728 during 1960–2008, exceeding the 99% confidence level. Although the correlation between the AO and NAO is very high, the relation between the AO/NAO and the Ural blocking may differ. In this section, we first survey the statistical relation between the

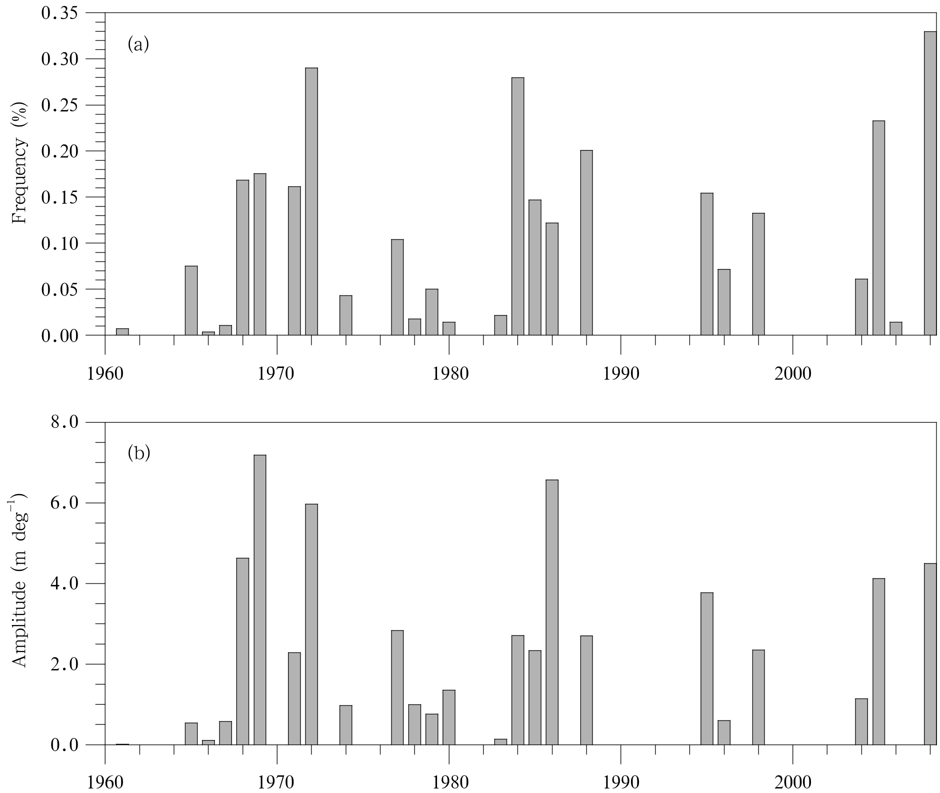

Fig. 1. Interannual variations of the Ural blocking high (a) frequency and (b) amplitude (unit: m deg^{-1}), using the TM90 blocking index.

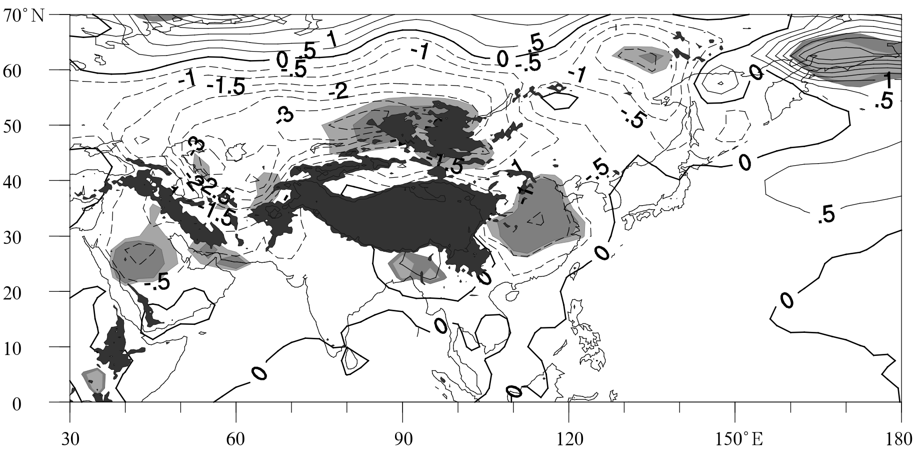

Fig. 2. Composite of January surface air temperature (SAT) anomalies (K) for the Ural blocking frequency greater than 0.16 (5 days). Light and dark shadings denote the regions that exceed the 90% and 95% confidence levels.

AO/NAO and the Ural blocking high in January and then discuss the situation in certain individual years.

4.1 The statistical relationship

In January, the 500-hPa geopotential height anomalies and the AOI exhibit a negative correlation coefficient of approximately –0.7 in the polar areas, related to the polar vortex (Fig. 3a). In the midlatitude area, there exists a positive correlation band with a maximum coefficient value of approximately 0.6. The positive correlation band has two large-value centers over the northern Atlantic Ocean and northern Pacific

Ocean, which coincide with the two main sectors of blocking activities associated with the storm track over the oceans. The band breaks up over Eurasia and North America. This distribution of correlation reflects the zonal land-sea thermal contrast. A negative correlation center over the Ural Mountains extends to the polar areas. The 500-hPa geopotential height anomaly over the Ural Mountains is positive during the negative AO phase, possibly favoring the blocking high activity, and vice versa.

We also investigated the relationship between the AO and the Ural blocking using the TM90 blocking index. When the AOI is greater than 0.6σ (standard deviation), a positive-AO-anomaly month is defined, and when less than -0.6σ, a negative-AO-anomaly month is defined. According to this criterion, a total of 10 (15) positive- (negative-) anomaly months is defined during 1960–2008 (Table 1). The average URBF and URBA in the negative- (positive-) AO-anomaly month are 0.056 and 1.28 m deg^{-1} (0.002 and 0.013 m deg^{-1}), respectively. The difference of URBF (URBA) between the negative and positive AO phases exceeds the 99% (98%) confidence level. The preceding analyses indicate that the Ural blocking high tends to be more persistent and tense during the negative AO phase than during the positive phase, which is consistent with the finding of Li and Gu (2010).

Table 1. January AO anomaly years during 1960–2008

AO(+)	1962, 1973, 1975, 1983, 1989, 1990 1993, 2000, 2002, 2007
AO(–)	1960, 1961, 1963, 1965, 1966, 1969, 1970, 1977, 1979, 1980, 1985, 1987, 1996, 1998, 2004

The threshold for the selection is the absolute value of AOI greater than 0.6σ (standard deviation).

Figure 3b depicts the correlation of the January NAO index and 500-hPa geopotential height anomalies. A dipole pattern of correlation with the maximum centers over the northern Atlantic Ocean and a zonal asymmetric structure are shown. The negative center over Greenland represents the IL, and the positive center over the northern Atlantic Ocean (40°N) represents the AH. The IL center at 500 hPa is located over Greenland, consistent with that in Ulbrich and Christoph (1999). In addition, a weaker secondary dipole is located over the downstream of the northern Atlantic Ocean. The weaker dipole exhibits a positive center north of the Urals and a negative center south of the Urals which is not statistically significant. The relative low correlation coefficient over the Urals (60°N, 60°E) indicates that the relationship between the NAO and the circulation over this sector is not very close statistically. From the preceding correlation analyses, the activity of the Ural blocking appears closely related to the different phases of the AO.

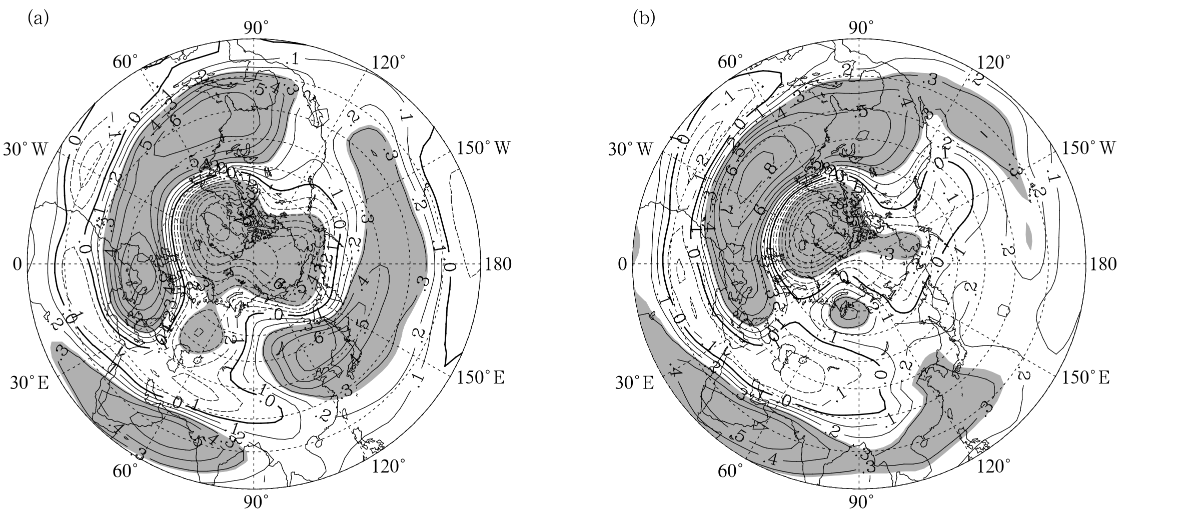

Fig. 3. Distributions of the correlation between (a) AO, (b) NAO and 500-hPa geopotential height anomalies (in gpm) in January of 1960–2008. Contour intervals are 0.1, and the shadings denote regions that exceed the 95% confidence level.

4.2 The eastward extending of the IL and the Ural blocking

A severe freezing rain and snow storm attacked southern China in January 2008. One of the main causes of the "0801" event is the activity of blocking over the Urals. The center of the positive height anomaly related to the Ural blocking high (UR) was located at 65°N, 60°E (Fig. 4), a slight northward shift from the climatological location of the center of the Ural blocking (60°N). In January 2008, the Ural blocking occurred while the AO was in a positive period (hereafter referred to as a positive UR-AO event for brevity). Li and Gu (2010) indicated that the situation for January 2008 does not align with the statistical relationship between the AO and the UR. In contrast, there are some years in the negative AO phase in which height anomalies over the Urals are negative (negative UR-AO events, hereafter).

Table 2 lists the UR-AO events during 1960–2008. One criterion for the UR-AO events is an absolute value of UHI greater than 40 gpm. The average value of URBF is 0.261 for positive UR-AO events, indicating that the blocking is very persistent. On the contrary, no blocking event is detected in the negative AO-UR events using the TM90 blocking index.

Figure 5 illustrates the composites of 500-hPa geopotential height anomalies for the two groups of

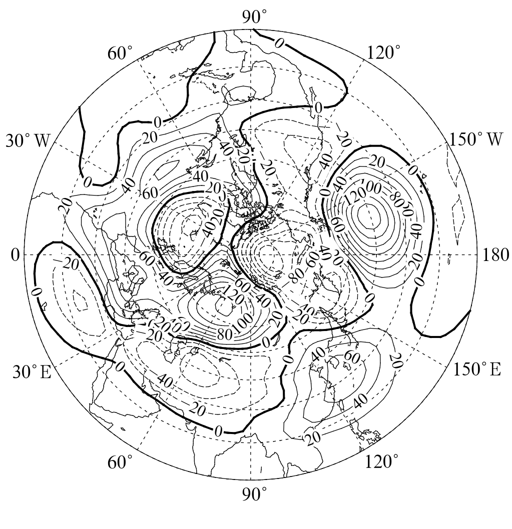

Fig. 4. Monthly mean 500-hPa geopotential height anomalies (units: gpm) in January 2008. Contour intervals are 20 gpm.

UR-AO events and shows an asymmetrical zonal structure of the atmospheric circulation. The significant signatures are mainly concentrated over the Ural Mountains and the northern Atlantic Ocean, with insignificant anomalies over the northern Pacific Ocean. The common feature of both positive and negative UR-AO events is that the IL exhibited eastward extending. Originally, the climatological center of the IL is located over Greenland at 500 hPa (see Fig. 3b). When the center of the IL shifted to east of 30°W, the NAO dipole anomaly pattern in upstream region exhibited a northeast-southwest tilting and exerted more impacts on the UR occurrence, undermining the statistical relationship between the AO and the UR. The AH, IL, and the anomaly center over the Urals exhibit poleward (equatorward) tilting wave-train-like characteristics in the positive (negative) UR-AO events. The case of the Ural blocking in January 2008 (Fig. 4) matches the composite of the positive UR-AO events. Additionally, the centers of 500-hPa geopotential height anomalies over the Urals in two groups exhibit slight differences. The anomaly center in the positive UR-AO events is located around 65°N, 60°E, and the counter center in the negative UR-AO events is located around 55°N, 45°E.

The eastward extending of the center of the IL and the blocking high over Eurasia in January 2008 can also be presented in a synoptic view. Luo et al. (2007) noted that the positive-phase NAO favors the occurrence of European blocking events. Consistent with this result, a pre-existing anticyclonic anomaly occurred over Scandinavia/western Russia from late December 2007 to early January 2008 (Bueh et al., 2011). Bueh et al. (2011) analyzed the processes of a European blocking extending eastward by using transient eddy feedback forcing. During January 2008, four heavy precipitation events occurred (Tao and Wei, 2008). The eastward shift of the center of the IL and the blocking high in the first precipitation event were the most prominent. Figure 6a indicates that the blocking was over the European continent (30°E) and the center of IL was located west of 30°W on 1 January 2008. Afterward, the blocking extended eastward to the Urals (60°E), and the center of the IL shifted east of 30°W on 7 January 2008 (Fig. 6b). The eastward extending of the center of the IL was also associated with the reconstruction of the blocking high around the Urals in the subsequent three precipitation episodes in January 2008 (figure omitted).

Table 2. Quantitative characteristics of the two groups of UR-AO events

Positive UR-AO events					Negative UR-AO events				
Year	AOI	NAOI	URBF	UHI	Year	AOI	NAOI	URBF	UHI
1984	0.905	1.66	0.28	95.7	1982	−0.883	−0.89	0	−55.3
1988	0.265	1.02	0.201	43.7	1987	−1.148	−1.15	0	−70.0
2005	0.356	1.52	0.233	47.7	1997	−0.457	−0.49	0	−120.5
2008	0.819	0.89	0.33	75.7					

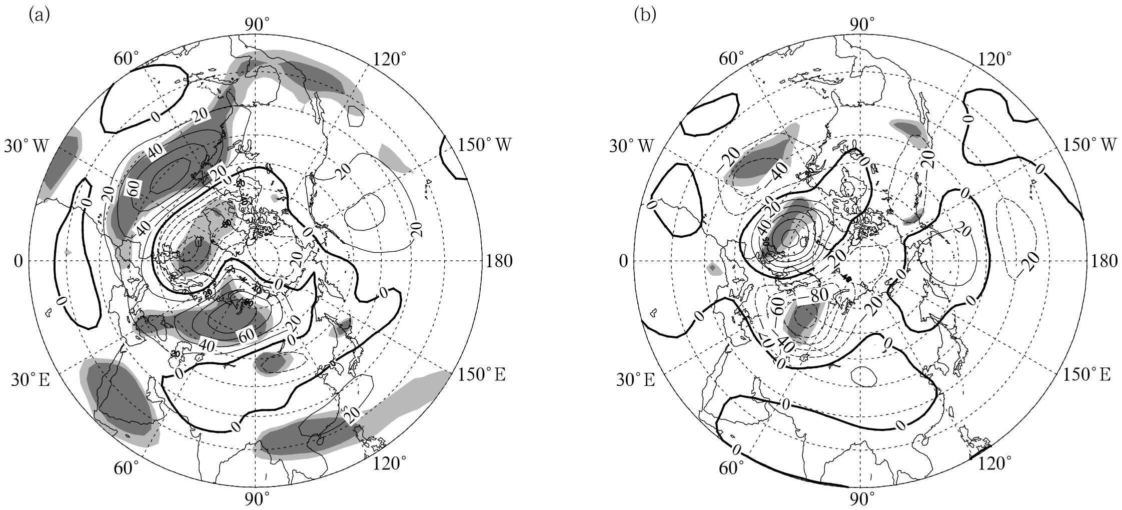

Fig. 5. Composites of January 500-hPa geopotential height anomalies for the (a) positive and (b) negative UR-AO events. Contour intervals are 20 gpm. Light and dark shadings denote regions that exceed the 90% and 95% confidence levels.

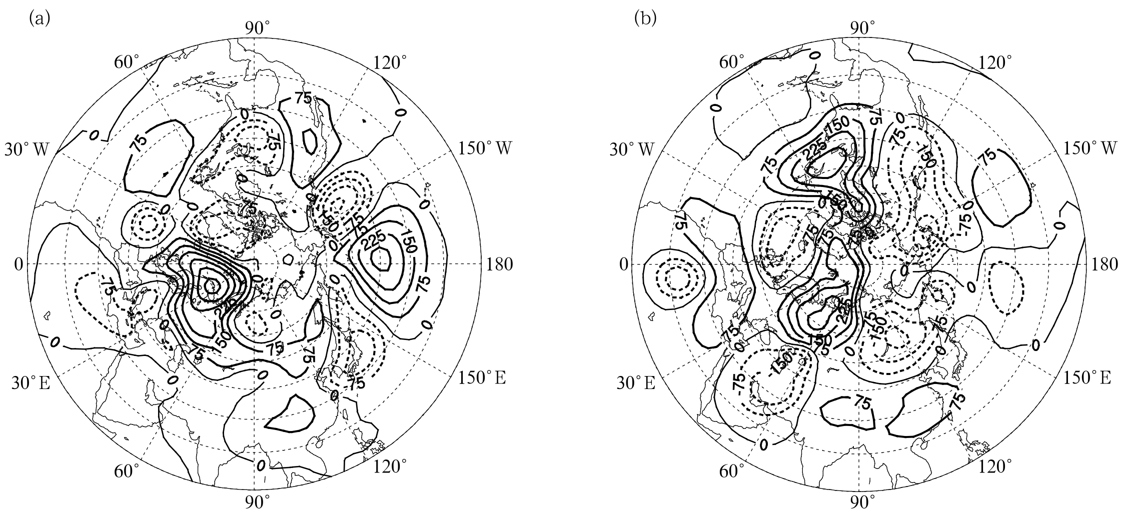

Fig. 6. Daily 500-hPa geopotential height anomaly fields on (a) 1 and (b) 7 January 2008. Contour intervals are 75 gpm.

5. The NAO anomaly pattern and quasi-stationary planetary wave

From the preceding analyses, we can see the importance of the eastward shift of the IL and the associated NAO dipole anomaly pattern in the upstream region for the activity of the Ural blocking in the UR-AO events. The cause and effect of the eastward shift of the IL center are also noteworthy.

The cause of the eastward shift of NAO center has been widely discussed in previous studies. Ulbrich and Christoph (1999) argued that increasing greenhouse gas concentrations are the main cause for the eastward shift of the center of action of the observed NAO pattern. Peterson et al. (2003) noted that this eastward shift may be due to an increase in the strength of the mean westerly wind in the Atlantic basin. Luo and Gong (2006) confirmed that in a strong mean westerly wind, the mean flow-induced eastward shift of the NAO exceeds the eddy-induced westward shift so that the NAO anomaly can undergo a net eastward shift.

Recently, Luo et al. (2010a, b) indicated that the meridional distribution of the jet may contribute to the NAO dipole anomaly pattern according to the dynamical analytical solution and numerical model experiments. An initial symmetric dipole anomaly in the meridional direction can evolve into a northeast-southwest (NE-SW) or northwest-southeast (NW-SE) tilted dipole structure if the core of this jet is in higher latitudes (the north) or in lower latitudes (the south). The results predicted by the linear Rossby wave theory in slowly varying media also confirm this. Climatologically, the maximum westerly wind core over the North Atlantic Ocean occurs at 45°N (figure omitted), deducing a faster zonal phase speed of the NAO dipole in midlatitudes than in high latitudes. Such a phase speed distribution causes the NW-SE pattern of the NAO. The core of the northward (southward) jet shift can cause the zonal wind to intensify (weaken) in high latitudes and to weaken (intensify) in midlatitudes (see Fig. 1 in Luo et al., 2010b).

Figure 7 illustrates the January zonal wind at 500 hPa over the North Atlantic (60°W–0°). The solid line in Fig. 7a (Fig. 7b) represents the mean zonal wind of the positive (negative) AO anomaly months in Table 1. The mean zonal wind in high latitudes (40°–60°N) of the positive UR-AO events is larger than the mean of the AO anomaly months with stronger baroclinity. On the contrary, the mean zonal wind in midlatitudes (20°–40°N) of the positive UR-AO events is smaller than the mean of the AO anomaly months with relaxed baroclinity, and the alteration latitude is approximately 40°N. The meridional distribution of zonal wind of the positive UR-AO events may explain the eastward shift of the IL center and the NAO dipole anomaly pattern, according to the theory of Luo et al. (2010a, b). The negative AO phase is similar to the positive AO phase, except that the alteration latitude is approximately 44°N in the negative AO phase, higher than its counterpart in the positive UR-AO events. The meridional distribution of zonal wind over the North Atlantic in January 2008 (thin line in Fig. 7a) is identical to the mean of the positive UR-AO events. Thus, the anomaly of zonal wind in the Atlantic sector may explain the IL eastward shift, which is very important for the Ural blocking high activity in January 2008.

We further examine zonal wind at 500 hPa over the Eurasian sector (20°–90°E, Fig. 8). The most prominent differences of zonal wind between the UR-AO events and the mean of corresponding AO anomaly months in Table 1 occur primarily in midlatitudes. The larger mean zonal wind in high latitudes (64°–80°N) and the smaller one in midlatitudes (40°–64°N) of the positive UR-AO events (Fig. 8a) induce greater phase speed and thus disperse more energy downstream to high latitudes. This distribution of basic flow coincides with the poleward tilting wave-train-like anomaly chain in the positive UR-AO events. The meridional distribution of basic flow of the negative UR-AO events (Fig. 8b) is opposite to the positive UR-AO events. The mean zonal wind of the negative UR-AO events is greater in midlatitudes (40°–60°N). More energy disperses downstream to midlatitudes, which coincides with the equatorward tilting wave-train-like anomaly chain in the negative UR-AO events. The situation for January 2008 is more prominent than the mean of the positive UR-AO events,

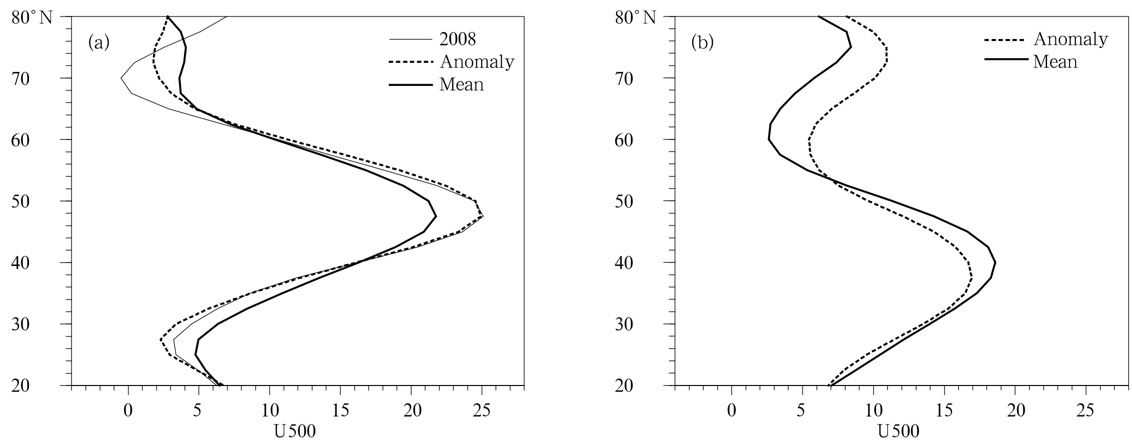

Fig. 7. Meridional distributions of January zonal wind at 500 hPa (U500) in the Atlantic sector (60°W–0°) for (a) positive AO phase and (b) negative AO phase. Solid and dashed lines represent the mean of AO anomaly months in Table 1 and the UR-AO events during 1960–2008, respectively. The thin solid line in (a) is for January 2008.

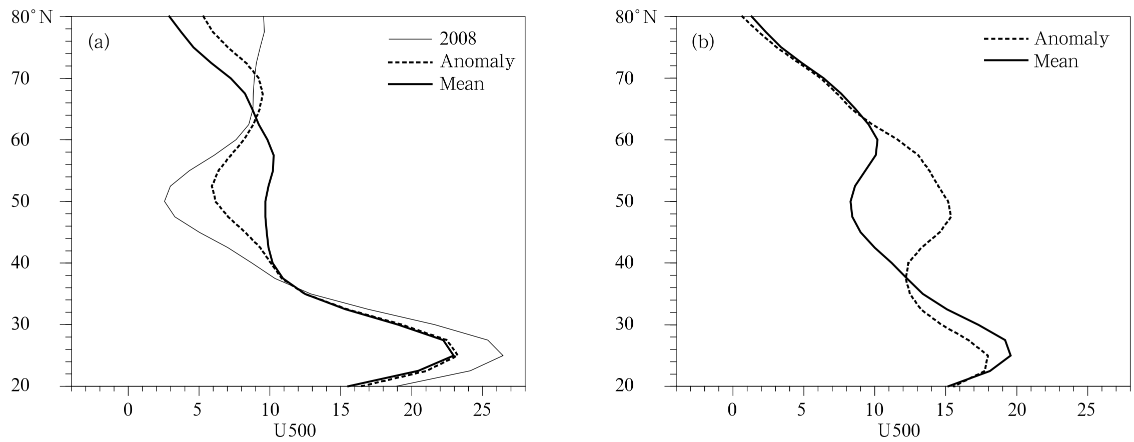

Fig. 8. As in Fig. 7, but for the meridional distributions of January zonal wind in the Eurasian sector (20°–90°E).

explaining the poleward shift of the Ural blocking high center to 65°N (Fig. 4).

The effect of eastward shift of the IL on the Ural blocking was examined from the perspective of quasi-stationary planetary waves. Figure 9 shows the anomalous amplitude of quasi-stationary planetary waves for the two groups of UR-AO events. Wavenumber 2 at 60°N at 500 hPa in the positive UR-AO events is significantly strengthened, and wavenumber 3 is weakened accordingly. The half wavelength is approximately 90 degrees for wavenumber 2. While the center of the IL in the upstream region shifts eastward to 30°W, the strengthened wavenumber 2 explains the positive height anomaly over the Urals with the center at 60°E. The situation is different in the negative UR-AO events. Wavenumber 3 is significantly strengthened, and wavenumber 2 is weakened in the negative UR-AO events. The half of wavelength is approximately 60 degrees for wavenumber 3. The shortened wavelength accounts for the negative height anomaly over the Urals with the center located near 45°E. The situation of the activity of the Ural blocking in January 2008 is the same as the positive UR-AO events. The eastward shift of the IL and the anomalous quasi-stationary planetary waves are responsible for the circulation anomalies over the Urals in the two groups of UR-AO events.

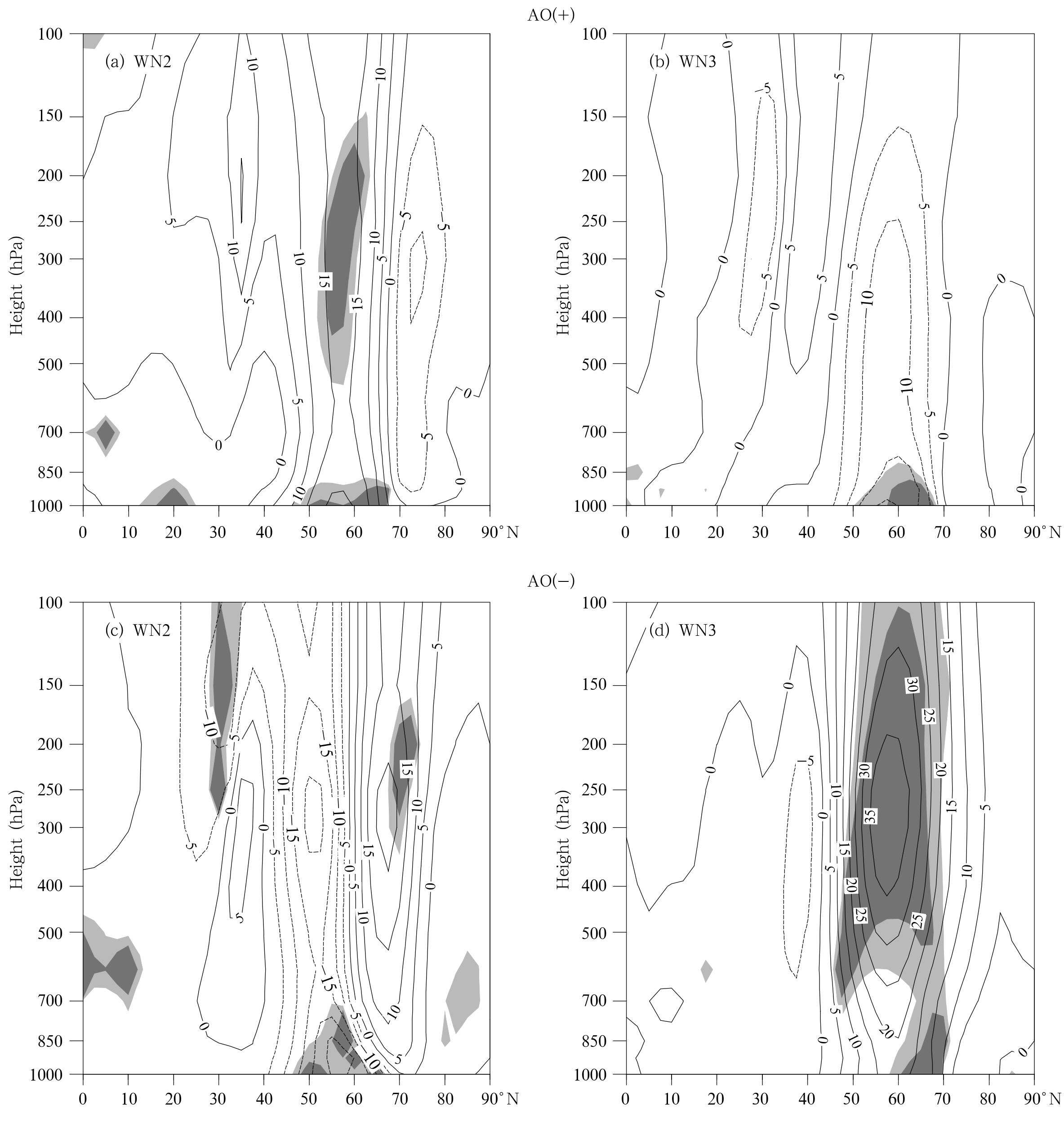

Fig. 9. Composites of January amplitude anomalies of the quasi-stationary planetary waves for wavenumbers 2 (a) and 3 (b) in positive UR-AO events, and for wavenumber 2 (c) and 3 (d) in negative UR-AO events. Contour intervals are 5 gpm. Light and dark shadings denote regions that exceed the 90% and 95% confidence levels.

6. Summary and discussion

Based on the NCEP-NCAR reanalysis data, the interannual variations of the Ural blocking high and associated impact on the East Asian climate in January have been investigated. The surface air temperature is lower than normal due to the activity of the Ural blocking. One of the main causes of the severe snowstorms in China during January 2008 is the persistent maintanence of the Ural blocking high.

To investigate the interannual variability of the Ural blocking, its relation to the AO/NAO was also analyzed. The Ural blocking high tends to be more frequent and tense during the negative AO phase than during the positive AO phase, according to the statistical analyses. The relationship between the AO and the Ural blocking does not fit in some abnormal years, including January 2008.

We focused not only on the index and phase of the AO/NAO but also on the structure of the teleconnections. The zonal asymmetric structure of the AO may play a more important role in the UR-AO events. The significant features in the composites of 500-hPa geopotential height anomalies are mainly over the Urals and the northern Atlantic Ocean. The anomalies over the northern Pacific Ocean are not significant. The atmospheric circulation in the UR-AO events exhibits more NAO dipole anomaly patterns. The center of the IL in the upstream region extends east of 30°W, and the NAO dipole shows a northeast-southwest anomaly pattern in the UR-AO events. The influence of anomalous location of the IL on the Ural blocking is investigated from the perspective of quasi-stationary planetary waves. While the center of the IL extends eastward to 30°W in the upstream, the strengthened amplitude of zonal wavenumber 2 (wavenumber 3) explains the positive (negative) 500-hPa geopotential height anomalies at 60°E (45°E) in the positive (negative) UR-AO events that favor (suppress) the activity of the Ural blocking. The situation of the Ural blocking in January 2008 matches the positive UR-AO events.

As being noted, the NAO and the Ural blocking high are both nonlinear problems. Some previous studies have considered the interaction between basic flow, planetary waves, and synoptic-scale eddies (Luo et al., 2005, 2010c). We use the theory of Luo et al. (2010a, b) that assumes the scale separation to explain the anomaly patterns of the NAO and the Ural blocking high. The enhanced zonal wind with stronger baroclinity in high latitudes and attenuated zonal wind with relaxed baroclinity in midlatitudes over the North Atlantic render the eastward shift of the center of the IL, according to the theory of Luo et al. (2010a, b). Intensified zonal wind in high latitudes and weakened zonal wind in midlatitudes in the Eurasian sector render the poleward tilting wave-train-like anomaly chain in the positive UR-AO events and explain the poleward shift of the Ural blocking in the positive UR-AO events. The distributions of zonal wind in the Eurasian sector correspond to the equatorward tilting wave-train-like anomalies chain in the negative UR-AO events. Thus, the NAO dipole anomaly pattern and the anomalous quasi-stationary planetary waves are responsible for the circulation anomalies over the Urals in the two groups of UR-AO events.

The analyses in this study are based on the January monthly mean. In fact, the interannual variations of the Ural blocking can also be revealed by the means of winter (December-January-February). Wang et al. (2010) noted that the Ural blocking underwent an eastward shift after 1976/1977, and the NAO pattern simultaneously exhibited an eastward shift (Hilmer and Jung, 2000). The interdecadal relationship between the Ural blocking and the NAO anomaly pattern in the upstream also deserves further discussion. This study focuses on the internal atmospheric variations, such as the AO/NAO, quasi-stationary waves and their effects on the Ural blocking. Some studies also indicate that external forcing, such as sea surface temperature anomalies (SSTA) in the Atlantic Ocean and snow mass, can modulate the AO/NAO pattern (Gong et al., 2002; Li et al., 2007). Therefore, external factors, such as ocean or land processes, should be considered in a general circulation model in the future.

Acknowledgments. The authors thank two anonymous reviewers for their valuable comments and suggestions. Thanks also go to Prof. Dehai Luo and Prof. Cholaw Bueh for many interesting discussions during the course of this work.

REFERENCES

Barnston, A., and R. Livezey, 1987: Classification, seasonality and persistence of low-frequency atmospheric circulation patterns. *Mon. Wea. Rev.*, **115**(6), 1083–1126.

Barriopedro, D., R. García-Herrera, A. R. Lupo, et al., 2006: A climatology of Northern Hemisphere blocking. *J. Climate*, **19**(6), 1042–1063.

Bueh, C., N. Shi, and Z. Xie, 2011: Large-scale circulation anomalies associated with persistent low temperature over southern China in January 2008. *Atmos. Sci. Lett.*, **12**(3), 273–280, doi: 10.1002/asl.333.

Chen, W., S. Yang, and R. H. Huang, 2005: Relationship between stationary planetary wave activity and the East Asian winter monsoon. *J. Geophys. Res.*, **110**, D14110, doi:10.1029/2004JD005669.

Dole, R. M., and N. Gordon, 1983: Persistent anomalies of the extratropical Northern Hemisphere wintertime circulation: Geographical distribution and regional persistence characteristics. *Mon. Wea. Rev.*, **111**(8), 1567–1586.

——, 1986: Persistent anomalies of the extratropical Northern Hemisphere wintertime circulation: Structure. *Mon. Wea. Rev.*, **114**(1), 178–207.

Gong, D. Y., S. W. Wang, and J. H. Zhu, 2001: East Asian winter monsoon and Arctic oscillation. *Geophys. Res. Lett.*, **28**(10), 2073–2076, doi: 10.1029/2000GL012311.

Gong, G., D. Entekhabi, and J. Cohen, 2002: A large-ensemble model study of the wintertime AO-NAO and the role of interannual snow perturbations. *J. Climate*, **15**(23), 3488–3499.

Hilmer, M., and T. Jung, 2000: Evidence for a recent change in the link between the North Atlantic oscillation and Arctic sea ice export. *Geophys. Res. Lett.*, **27**(7), 989–992, doi: 10.1029/1999GL010944.

Kalnay, E., and Coauthors, 1996: The NCEP/NCAR 40-year reanalysis project. *Bull. Amer. Meteor. Soc.*, **77**(3), 437–471.

Li Chongyin and Gu Wei, 2010: An analyzing study of the anomalous activity of blocking high over the Ural Mountains in January 2008. *Chinese J. Atmos. Sci.*, **34**(5), 865–874. (in Chinese)

Li, S., 2004: Impact of Northwest Atlantic SST anomalies on the circulation over the Ural Mountains during early winter. *J. Meteor. Soc. Japan*, **82**(4), 971–988.

——, W. A. Robinson, M. P. Hoerling, et al., 2007: Dynamics of the extratropical response to a tropical Atlantic SST anomaly. *J. Climate*, **20**(3), 560–574.

Luo, D., 2005: A barotropic envelope Rossby soliton model for block-eddy interaction. Part I: Effect of topography. *J. Atmos. Sci.*, **62**(1), 5–21.

——, and T. Gong, 2006: A possible mechanism for the eastward shift of interannual NAO action centers in last three decades. *Geophys. Res. Lett.*, **33**, L24815, doi: 10.1029/2006GL027860.

——, A. R. Lupo, and H. Wan, 2007: Dynamics of eddy-driven low-frequency dipole modes. Part I: A simple model of North Atlantic oscillations. *J. Atmos. Sci.*, **64**(1), 3–28.

——, Z. Zhu, R. Ren, et al., 2010a: Spatial pattern and zonal shift of the North Atlantic oscillation. Part I: A dynamical interpretation. *J. Atmos. Sci.*, **67**(9), 2805–2826.

——, L. Zhong, R. Ren, et al., 2010b: Spatial pattern and zonal shift of the North Atlantic oscillation. Part II: Numerical experiments. *J. Atmos. Sci.*, **67**(9), 2827–2853.

——, J. Liu, and J. Li, 2010c: Interaction between planetary-scale diffluent flow and synoptic-scale waves during the life cycle of blocking. *Adv. Atmos. Sci.*, **27**(4), 807–831.

Park, T.-W., C.-H. Ho, and S. Yang, 2011: Relationship between the Arctic oscillation and cold surges over East Asia. *J. Climate*, **24**(1), 68–83.

Peterson, K. A., J. Lu, and R. J. Greatbatch, 2003: Evidence of nonlinear dynamics in the eastward shift of the NAO. *Geophys. Res. Lett.*, **30**(2), 1030, doi: 10.1029/2002GL015585.

Rex, D., 1950: Blocking action in the middle troposphere and its effect upon regional climate. *Tellus*, **2**(4), 275–301.

Sumner, E., 1954: A study of blocking in the Atlantic-European sector of the Northern Hemisphere. *Quart. J. Roy. Meteor. Soc.*, **81**(345), 402–416.

Tao Shiyan, 1957: A synoptic and aerological study on a cold wave in the far east during the period of the break down of the blocking situation over Euroasia and Atlantic. *Acta Meteor. Sinica*, **28**(1), 63–74. (in Chinese)

—— and Wei Jie, 2008: Severe snow and freezing rain in January 2008 in South China. *Climatic Environ. Res.*, **13**(4), 337–350. (in Chinese)

Tibaldi, S., and F. Molteni, 1990: On the operational predictability of blocking. *Tellus*, **42**(3), 343–365.

Ulbrich, U., and M. Christoph, 1999: A shift of the NAO and increasing storm track activity over Europe due to anthropogenic greenhouse gas forcing. *Climate Dyn.*, **15**(7), 551–559.

Van Loon, H., R. Jenne, and K. Labitzke, 1973: Zonal harmonic standing waves. *J. Geophys. Res.*, **78**(21), 4463–4471.

Wallace, J., and D. Gutzler, 1981: Teleconnections in the geopotential height field during the Northern Hemisphere winter. *Mon. Wea. Rev.*, **109**(4), 784–812.

Wang, L., W. Chen, W. Zhou, et al., 2010: Effect of the climate shift around mid 1970s on the relationship between wintertime Ural blocking circulation and East Asian climate. *Int. J. Climatol.*, **30**(1), 153–158.

Wiedenmann, J. M., A. R. Lupo, I. I. Mokhov, et al., 2002: The climatology of blocking anticyclones for the Northern and Southern Hemispheres: Block intensity as a diagnostic. *J. Climate*, **15**(23), 3459–3473.

Wu, B., and J. Wang, 2002: Winter Arctic oscillation, Siberian high and East Asian winter monsoon. *Geophys. Res. Lett.*, **29**(19), 1897, doi: 10.1029/2002GL015373.

Ye Duzheng, Tao Shiyan, and Zhu Baozhen, 1962: *The Study on Wintertime Blocking Pattern of the Northern Hmisphere.* Chinese Science Press, 220 pp. (in Chinese)